Received: 26 August 2022 | Accepted: 16 April 2023

DOI: 10.1111/opo.13156

ORIGINAL ARTICLE

OPO THE COLLEGE OF OPTOMETRISTS

Role of instrumental factors in Meibomian gland contrast assessment

Elena Diz-Arias[1] | **Elena Fernández-Jiménez**[2] | **Assumpta Peral**[2] | **Jose A. Gomez-Pedrero**[1]

[1]Optics Department, Faculty of Optics and Optometry, University Complutense of Madrid, Madrid, Spain

[2]Department of Optometry and Vision, Faculty of Optics and Optometry, University Complutense of Madrid, Madrid, Spain

Correspondence
Elena Diz-Arias, Optics Department, Faculty of Optics and Optometry, University Complutense of Madrid, Madrid, Spain.
Email: elenadiz@ucm.es

Funding information
European Fund for Regional Development; Santander-UCM grant for pre-doctoral research students; Spanish Government´s Agencia Estatal de Investigación, Grant/Award Number: DPI2016-75272-R

Abstract

Purpose: Meibomian gland contrast has been suggested as a potential biomarker in Meibomian gland dysfunction. This study analysed the instrumental factors related to contrast. The objectives were to determine whether the mathematical equations used to compute gland contrast (e.g., Michelson or Yeh and Lin), impact the ability to identify abnormal individuals, to ascertain whether contrast between the gland and the background could be an effective biomarker and to assess whether using contrast-enhancement on the gland image improves its diagnostic efficacy.

Methods: A total of 240 meibography images from 40 participants (20 controls and 20 having Meibomian gland dysfunction or blepharitis), were included. The Oculus Keratograph 5M was used to capture images from the upper and lower eyelids of each eye. The contrast of unprocessed images and those pre-processed with contrast-enhancement algorithms were analysed. Contrast was measured on the eight central glands. Two equations for contrast computation were used, and the contrast both between glands and within a gland were calculated.

Results: Significant differences were found between the groups for inter-gland area in the upper ($p = 0.01$) and lower eyelids ($p = 0.001$) for contrast measured with the Michelson formula. Similar effects were observed when using the Yeh and Lin method in the upper ($p = 0.01$) and lower eyelids ($p = 0.04$). These results were obtained for images enhanced with the Keratograph 5M algorithm.

Conclusions: Meibomian gland contrast is a useful biomarker of disease related to the Meibomian glands. Contrast measurement should be determined using contrast-enhanced images in the inter-gland area. However, the method used to compute contrast did not influence the results.

KEYWORDS
biomarker, contrast, meibography, Meibomian gland dysfunction, Meibomian glands

INTRODUCTION

Meibomian glands (MGs) are sebaceous glands located on the tarsal plates of each eyelid. They are composed of secretory groups of acini connected through small ducts to a long central duct that runs along the tarsal plate and ends at the free edge of the eyelid. These structures create and transport lipids (meibum) to the tear film. Meibum, the main component of the tear lipid layer, acts to maintain stability and prevent excessive evaporation of the tear fluid.[1] Changes in the MG may result in reduced production of meibum, and modification of the tear film leads to multifactorial diseases associated with these glands, e.g., Meibomian gland dysfunction (MGD) and dry eye disease.

Therefore, it is important to perform a structural and functional evaluation of the MGs to allow an early and

accurate diagnosis of related pathology.[2] This evaluation comprises a battery of diagnostic objective and subjective tests for MG-related conditions.[3,4] It should include both symptomatology (using questionnaires such as the Ocular Surface Disease Index (OSDI),[5] Visual Analogue Scale (VAS),[6] Contact Lens Dry Eye Questionaire (CLDEQ),[4] Meibomian Gland Dysfunction 14[7] (MGD-14)) and clinical tests, including tear film breakup time, corneal and conjunctival staining, evaluation of eyelid morphology as well as the expression and quality of the meibum.[4]

Additionally, in vivo visualisation of the MG is conducted to allow morphological investigation using meibography. Using specialised lighting, the glands (acini and ducts) are observed as highly reflective (bright) areas, while the inter-gland zones appear as areas of low brightness.

Non-contact meibography is the most widely used procedure[2,8,9] as described by Arita et al.[10] An infrared filter is coupled to a slit lamp and video camera to obtain images. This procedure is both simple and fast and provides minimal discomfort to the patient.[2,9]

Meibographic images allow assessment of glandular loss, as well as providing information regarding the functionality of the glands.[9] Additionally, there are a number of subjective measurement techniques and grading scales, such as those described by Riede Pult et al.[11] and Arita et al.[12] Using these subjective techniques, the eye care professional can assess the severity of glandular loss.[13] Recently, objective methods for evaluating MGs have been reported. Image processing, machine learning and deep learning techniques are used to determine MG morphology. The goal of these techniques is the objective segmentation of the glands from the surrounding tissues within the everted eyelids. From this segmentation, the anatomical and physiological properties of the glands can be quantified as a metric.[14–17] Objective MG assessment methods show good inter and intra-observer repeatability, which makes them comparable with manual evaluation of MG morphology.[18–20]

Recent studies have reported that objective measurement of the contrast of the glands against the surrounding background, computed from the intensity levels on MG images may be a new indicator of pathology.[21,22] The anatomical structure of the MGs, consisting of bright glands spaced over a dark background, resembles a fringe pattern. Therefore, it is possible to define the contrast using Michelson's definition of fringe contrast, or visibility, as a percentage:

$$C = 100 \cdot \frac{I_{max} - I_{min}}{I_{max} + I_{min}}, \quad (1)$$

where I_{max} and I_{min} are the maximum (gland) and minimum (background) intensities, respectively (intensity is the digitalised exposure of the pixels in an image of the tarsal conjunctiva, and it is measured in grey levels). Michelson's contrast (equation 1), was used to characterise MG contrast by Peral et al.[23] However, Yeh and Lin defined gland contrast as:

Key points

- Objectively measured Meibomian gland contrast is a possible biomarker for pathology.
- There are significant limitations in the methodologies used to capture images of the Meibomian glands.
- The methods proposed by both Michelson and Yeh and Lin to quantify contrast are equally effective when using gland contrast as a pathological biomarker.

$$C = I_{max} - I_{min} \quad (2)$$

with I_{max} and I_{min} representing the maximum and minimum intensities, respectively.[22] Notice that for either of these equations, contrast is defined between the glands and the background (region within the glands). This contrast will be referred to here as the inter-gland contrast. It is also possible to define the contrast within the gland as described later in the manuscript.

Inter-gland contrast is dependent on the wavelength of the incoming light,[23] reaching its maximum value around 850 nm, as used by many commercial meibographers. Furthermore, this parameter has shown good specificity and sensitivity in diagnosing lipid-deficient dry eye.[22] Therefore, it appears that inter-gland contrast could be a useful biomarker in the diagnosis of MG pathology. However, there are a number of instrumental aspects of the contrast measurement that need to be addressed. In this work, it is proposed to assess these instrumental issues.

First, there are two separate ways of computing contrast, described by equations (1) and (2). Although these are related, it must be determined whether the two methods of calculation are equally able to differentiate between healthy eyes and those with MG pathology. Second, in the work of Peral et al. a custom meibographer with a highly sensitive camera was used, whereas Yeh and Lin used a commercial instrument, the Oculus Keratograph 5M™ (K5M) (en.oculus.de).[21,22] The software of the K5M allows the user to enhance the contrast of the gland image using an undisclosed image processing algorithm, and Yeh and Lin computed the contrast from these enhanced images. Therefore, it is of interest to determine the effect of the contrast enhancement, especially the algorithm used by K5M.

Finally, it would be useful to know whether the contrast within the gland, that is the contrast between the bright acini and the gland background (i.e., between neighbouring acini) could also be used as a biomarker of MG. In this work, this will be referred to as in-gland contrast to differentiate it from the inter-gland contrast defined above.

The present study aimed to assess those instrumental issues. Therefore, there were three separate goals: (1) to determine whether the method used to compute gland contrast influences the ability to differentiate healthy individuals from those with an MG abnormality, (2) to ascertain whether in-gland contrast is equally effective as a biomarker compared with inter-gland contrast and (3) to assess whether performing contrast enhancement on the MG image alters its effectivity as a biomarker.

METHODS

Meibography images from both eyelids of individuals with healthy MGs, as well as those with MG abnormalities were obtained with a K5M meibographer. From these images, contrast (both in-gland and inter-gland) was computed using custom software, both with and without processing of the images using a contrast enhancement algorithm.

Meibography images were obtained during an ongoing prospective study approved by the ethics committee of the Hospital Clínico San Carlos de Madrid C.P. EO4/DPI2016-75272-R-C.I. 16/550-E, and carried out at the Faculty of Optics and Optometry, University Complutense of Madrid, Spain. All the procedures adhered to the Declaration of Helsinki.

Participants were enrolled in the Faculty of Optics and Optometry at the University Complutense of Madrid and provided written consent after an explanation of the nature of the study. The participants were classified into two groups (control and pathology). The pathological group had two inclusion criteria: an OSDI score ≥ 15 and a diagnosis of MGD or blepharitis confirmed by a specialist.[5]

The diagnosis of MGD was made by a single ophthalmologist on the staff of the Clinic of Optometry at the Faculty of Optics and Optometry. This diagnosis was based on ocular symptoms, observation of the palpebral structures (tarsal conjunctiva, lid margin, eye lashes, eyelid vascularisation), meibography images and meiboscore.[4,13] The ophthalmologist verified that all participants with pathology presented signs and symptoms of dry eye and abnormal meibography, with a degree of glandular loss ≥25%, which is equivalent to grade 2 on Pult's scale.[11] The inclusion criteria for the control group were as follows: (1) no contact lens wear, (2) a score < 15 on the OSDI test and (3) no changes in the tarsal conjunctiva. Participants with ocular inflammation, using systemic medication or presenting with a disease that could impact ocular health and a history of eye trauma or surgery (including corneal refractive surgery) were excluded from the study, as were participants who did not meet the inclusion criteria for either group.

To calculate the sample size, values reported in the literature for similar studies were used, with an alpha risk of 0.05, a beta risk of 0.20 and a minimum difference between groups of three points. A minimum sample of 18 eyes for each group (control and pathology) was determined.[22] Therefore, a total of 20 eyes per group was included to provide statistical reinforcement. The data from the 40 participants, comprising the control and pathology groups, were taken from a larger study that included 65 participants, of whom 25 were contact lens wearers. However, contact lens wearers were excluded from this study, since it has been reported that the use of contact lenses for more than 2 years can alter the morphology and function of the MGs.[24] One image of the upper and lower lid of each participant was selected randomly for analysis.

Meibography

The K5M was used to perform meibography by capturing images of the upper and lower eyelids. For each participant, two images per eyelid were obtained. Contrast was calculated for the eight central glands. Of the two images captured, one was contrast-enhanced using the algorithm provided with the instrument software (K5M C), while the second image, denoted as the raw image (K5M R), was captured without contrast enhancement. Finally, a third image was obtained by applying another contrast-enhancement algorithm (a contrast-limited adaptive histogram equalisation [CLAHE] algorithm)[25] to the raw image (K5M RC), to examine the impact of the contrast enhancement algorithm in determining gland contrast.

Meimobian gland contrast measurement

Contrast measurement was carried out on the eight central glands. Contrast was calculated from the meibography images using a software application (app) written in MATLAB (mathworks.com).[26] Contrast was calculated as described by Peral et al.[23] However, the image pre-processing was modified using the following steps:

1. After loading the image of the eyelid, a region of interest (ROI) was determined manually by selecting a set of points defining the polygonal contour of the ROI, as shown in Figure 1a. A binary ROI mask was defined from this polygonal contour using MATLAB's 'roipoly' function.
2. Glare was removed by setting a glare threshold intensity, established by trial as $gth = \left(6\max(I) - \bar{I}\right)/7$, where $\max(I)$ and $\bar{I}$ are the maximum and mean intensity of the gland image within the ROI, respectively. Therefore, those pixels located within the ROI mask whose intensity I, was higher than g^{th} were removed by setting the value of the ROI mask as false.
3. After removing glare, an optional image pre-processing was performed. The application user can select a low-pass Gaussian filter to remove noise, and independently an adaptive histogram equalisation for contrast enhancement. Contrast enhancement was carried out using MATLAB's 'adapthisteq' function, which implements the contrast-limited adaptive histogram equalisation

(a)

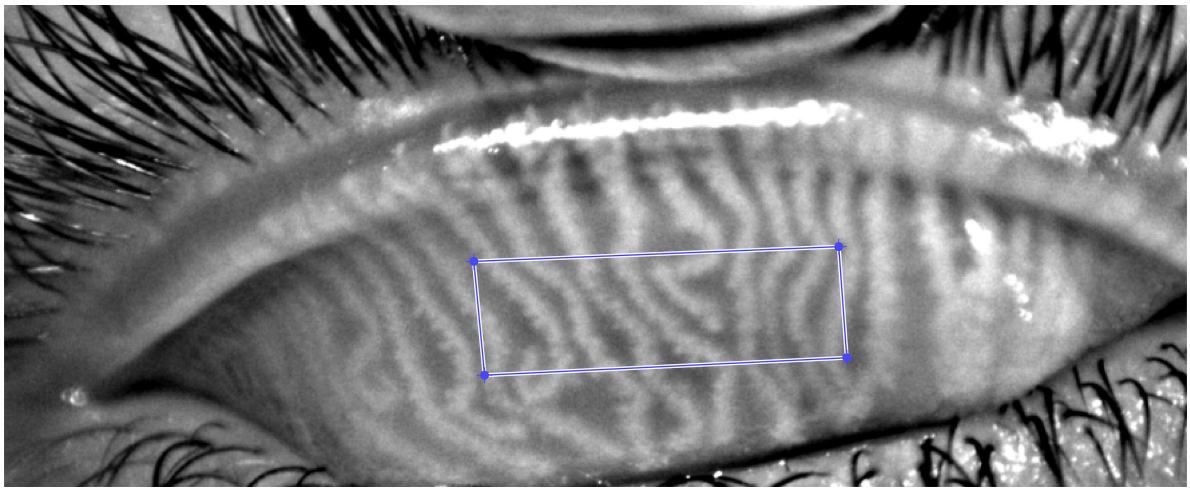

(b)

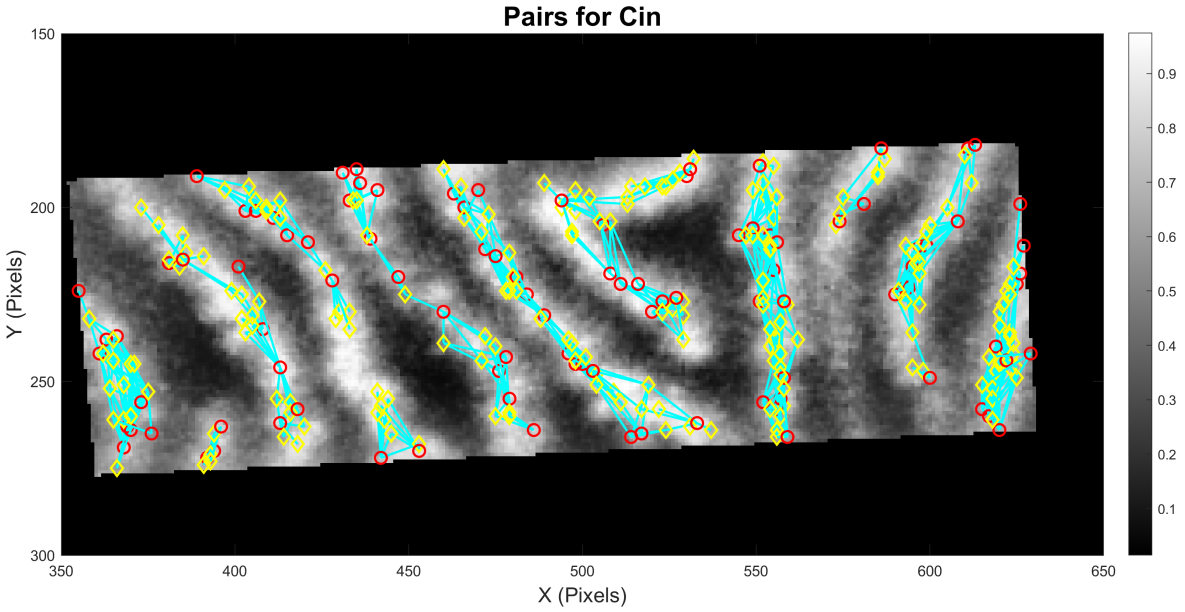

(c)

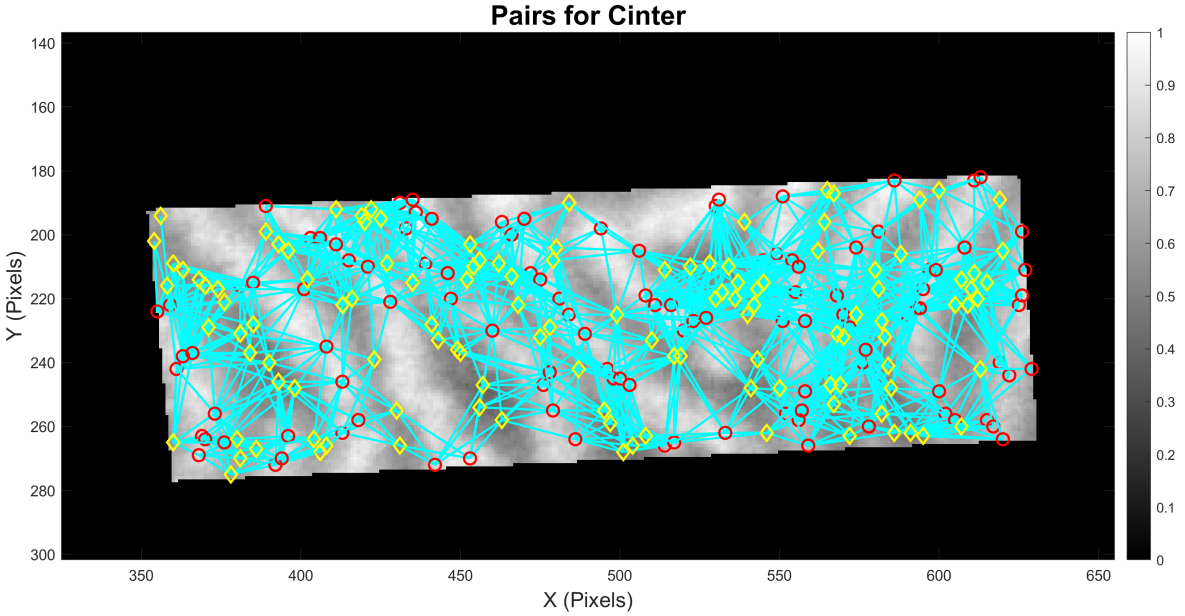

FIGURE 1 Oculus Keratograph 5M meibography with contrast enhanced by the device (K5M C). (a) Polygonal contour used to select a region of interest (ROI) comprising the eight central glands. (b) Local maxima (red circles) and minima (yellow diamonds) within the glands define the pairs for computing in-gland contrast. A cyan line joins each valid pair. (c) Local maxima (red circles) and minima (yellow diamonds) define the pairs for computing inter-gland contrast. Each valid pair is joined by a cyan line. The contrast in Figure 1b has been enhanced to show that all pairs are contained within a given gland. CIN, in-gland contrast; CINTER, inter-gland contrast.

(CLAHE) algorithm.[21] This step was applied to the raw images (K5M R) captured by this instrument to obtain the contrast-enhanced K5M RC images.

4. To distinguish the foreground objects (glands) from the background, Niblack's thresholding algorithm, using the implementation described by Senthilkumaran and Kirubakaran was employed.[27] This algorithm determines a local threshold for each pixel by combining the local mean and standard deviation of the neighbouring pixels.[27] By applying this threshold, and performing a logical union operation with the ROI mask obtained in the first step, a mask that distinguishes the MGs from the rest of the image was obtained.

After these pre-processing steps, the algorithm proceeded as described by Peral et al.[23] The goal was to compute both the in-gland and inter-gland contrast using the image of the eyelid plus the binary mask, separating the glands from the background. The app can calculate the contrast from either a contrast-enhanced image (K5M C) or a raw image (K5M R). In this latter case, the user can optionally generate a contrast-enhanced image using the CLAHE algorithm (K5M RC). In the following, the inter-gland contrast computed using Michelson equation (1) is termed CINTER. The in-gland contrast will be denoted as CIN and δCIN when calculated using the Michelson (equation 1) and Yeh and Lin (equation 2) methodologies, respectively.

Next, the algorithm for computing contrast is summarised, as detailed in Diz-Arias et al.[26] To calculate in-gland contrast, the algorithm computed a set of pixels within the gland that present maximum local intensity. It also identified the minimum local intensity pixels within a gland. The algorithm forms a set of pairs, with each pair combining a local maximum and minimum (both belonging to the same gland) and computes the contrast for each pair using either Michelson's (1) or Yeh and Lin's (2) equation. Finally, the in-gland contrast is calculated as the average contrast of the pairs. Figure 1b shows the pairs used when computing in-gland contrast for the rectangular region marked in Figure 1a. When computing inter-gland contrast, the algorithm proceeds in the same way, but here the pixels presenting minimum local intensities were located in the background area between the glands as shown in Figure 1c.

Figure 2 represents the distribution of in-gland and inter-gland contrasts, as measured from the pairs depicted in Figure 1b,c, respectively. As can be seen in this figure, the mean in-gland contrast is considerably lower[23] than the average inter-gland contrast.

Figure 3a shows a screen capture from the app before computing contrast, while Figure 3b depicts the result after calculating in-gland and inter-gland contrasts. The app is available on the web (https://github.com/InforUCM/ContrasteMG) and runs on MATLAB version 2021b (mathworks.com).[26] In addition to calculating gland contrast, the app can determine other morphological parameters, such as the relative gland length and the relative gland area. The first parameter is defined as the average length of the major axis of an elliptical area that best fits each gland divided by the width of the box that circumscribes the ROI. The second parameter is the quotient between the sum of the areas of the gland and the ROI area.

STATISTICAL ANALYSIS

For the statistical analysis, Microsoft Excel v.15.30 (Microsoft.com) and SPSS v.22.0 (IBM SPSS Statistics for Macintosh. Version 22.0; ibm.com) were used. Granmo calculator v.7.12 (imim.es/ofertadeserveis/software-public/granmo) was used to calculate the sample size. The normality of all datasets was tested with the Kolmogorov–Smirnov test. The non-parametric Mann–Whitney *U* test was used to compare contrast differences between the control and pathology groups.

RESULTS

A total of 40 eyes of 40 participants (20 control/20 pathology) were included in the study. Sex, age and clinical test scores are shown in Table 1. Significant differences were found for gender, with more women in the control group ($p = 0.03$). Statistically significant differences were also obtained for the OSDI scores between the groups, with a higher value in the pathology group ($p < 0.001$). Significant differences were observed for the VAS symptomatology test for symptoms of pain ($p = 0.03$), irritation ($p < 0.001$), burning ($p = 0.03$) and photophobia ($p < 0.001$); in all cases the dry eye symptoms were higher in the pathology group. The clinical tests showed significant differences between the groups for tear break up time ($p = 0.04$), bulbar conjunctival integrity ($p = 0.04$), lid margin irregularity ($p = 0.03$), telangiectasia ($p = 0.00$), meibum quality ($p = 0.02$) and meiboscores ($p < 0.001$). The clinical signs were poorer in the pathology group.

Analysis of MG contrast

The contrast of 120 meibography images, 40 K5M C, 40 K5M R and 40 K5M RC were analysed. The MG contrasts obtained show the following trends: In-gland (CIN) contrast

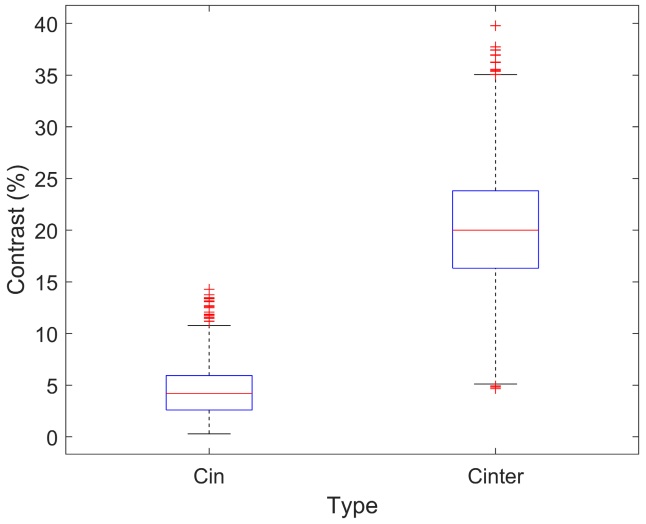

FIGURE 2 Boxplot representing the in-gland (Cin) and inter-gland (Cinter) Michelson contrast measured from the pairs represented in Figure 1b,c, respectively. Note that the mean inter-gland contrast was higher than the mean in-gland contrast, with greater dispersion.[23]

quantified using the Michelson method was equivalent for both groups. However, δCIN determined using the Yeh and Lin method was slightly lower in the pathology group. The inter-gland (CINTER) contrast was lower in the pathology group for all images (K5M C, K5M R and K5M RC) when determined using either the Michelson or Yeh and Lin methods. These results are shown in Table 2.

Given the number of comparisons presented in Table 2, it was important to verify that this was not due to a type I error (false positive). Therefore, the joint probability of the statistically significant comparisons was checked. Assuming statistical independence, if this joint test probability is reasonably high (i.e., close to 1), then it can be assumed that these results are correct. In fact, the assumption of statistical independence may be too strong here, since one might expect a significant correlation between the Michelson and Yeh and Lin contrast measures for the same eyelid and image preprocessing, given the similarity of equations (1) and (2).

Therefore, the joint probability of the comparisons in Table 2 where statistically significant differences between the groups were observed has been calculated using the following expression:

$$P_J = \prod_i \left(1 - p_i\right)_{i=1,2,\ldots N} \quad (3)$$

where P_J is the joint probability of the test, p_i the statistical significance level for each significant test and N *is* the number of significant tests, which from Table 2 was ten. The value obtained was $P_J = 0.824$, that is, very close to 1, indicating that the significant tests have a high probability of being true so that no further correction factor was needed.

Regarding in-gland contrast, statistically significant differences were found between the control and pathology groups. CIN contrast values for the pathology group were

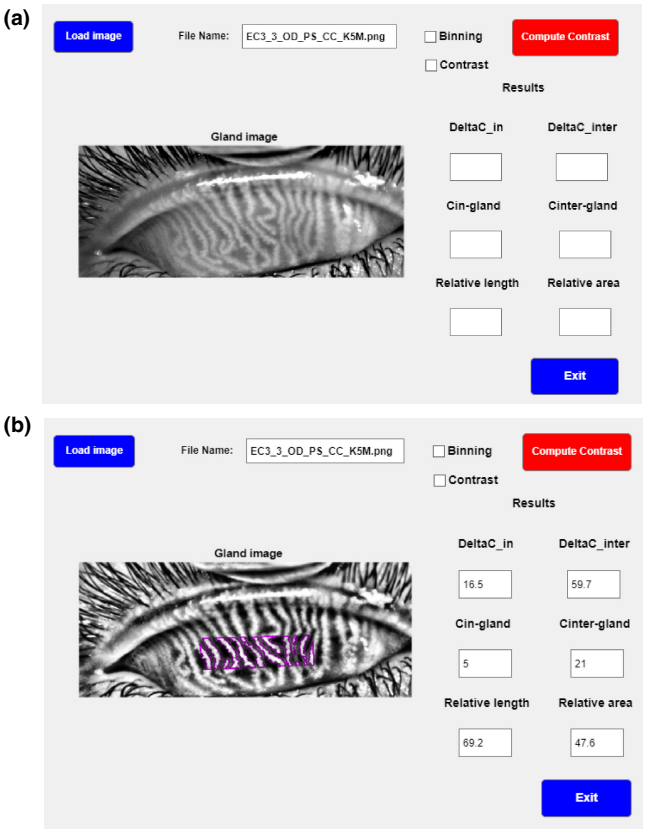

FIGURE 3 (a) Capture of the application window before processing a loaded image. (b) The same image after processing a region of interest (ROI) enclosing the central eight glands. DeltaC_in and DeltaC_inter represent the in-gland (δCIN) and inter-gland (δ CINTER) contrast computed using the method of Yeh and Lin (equation 2). Cin-gland and Cinter-gland are the in-gland (CIN) and inter-gland (CINTER) contrasts determined using the Michelson method (Equation 1) and expressed as a percentage. For illustrative purposes, the contrast of the gland image is enhanced in (b), although the contrast value was computed from the original image shown in (a), which was already a contrast-enhanced image provided by Keratograph 5M.

lower than the control group in the lower eyelid for the K5M C ($p = 0.02$) and K5M RC ($p = 0.004$) images using the Michelson equation. For the Yeh and Lin calculation, statistically significant differences were obtained for the δCIN variable, with the contrast being lower in the pathology group than the controls for the K5M RC images ($p = 0.03$) in the lower eyelid and the K5M R images ($p = 0.05$) in the upper eyelid.

For the inter-gland Michelson CINTER variable, significant differences were found between the groups for the lower eyelid K5M C ($p = 0.001$) and K5M RC ($p = 0.007$) images, with the contrast in the pathology group always being lower than the controls. CINTER contrast determined from the upper eyelid K5M C images of the pathology group was significantly lower than the control ($p = 0.01$). For the δCINTER variable (Yeh and Lin method), significant differences between the groups were observed in the lower eyelid for the K5M C ($p = 0.04$) and K5M RC ($p = 0.01$) images, as well as for K5M C in the upper eyelid ($p = 0.01$). In all these cases the δCINTER contrast was lower for the pathology group (see Table 2).

TABLE 1 Summary of demographic characteristics and clinical results obtained for the control and pathology groups.

	Control [$n = 20$; 40 eyelids] mean (SD)	Pathology [$n = 20$;40 eyelids] mean (SD)	p-Value
Sex Male/female	2/18	8/12	0.03*
Age Mean (SD)	27.9 (2.18)	37.3 (14.54)	0.06
Clinical test			
Ocular surface disease index (range 0–100)	8.60 (3.70)	32.5 (18.3)	<0.001 *
Visual analogue scale (range 0–100)			
Pain	6.9 (15.6)	7.2 (15.0)	0.03*
Dry eye sensation	25.3 (27.6)	44.3 (32.6)	0.08
Irritation	13.0 (23.8)	36.0 (27.8)	<0.001*
Burning	11.0 (27.4)	21.4 (26.3)	0.03*
Itching	18.2 (25.4)	27.7 (29.3)	0.26
Photophobia	15.2 (22.9)	39.4 (23.8)	<0.001*
Foreign body sensation	13.5 (19.0)	26.8 (31.7)	0.10
Visual acuity (LogMAR)	0.1 (0.2)	0.1(0.1)	0.45
Meniscus (μm)	0.2 (0.1)	0.2 (0.1)	0.61
Tear break-up time (seconds)	5.2 (1.8)	4.0 (1.8)	0.04*
Corneal integrity assessment (range 0–15)	0.8 (0.8)	1.2 (2.3)	0.80
Bulbar conjunctival integrity (range 0–18)	2.0 (1.9)	4.7 (4.1)	0.04*
Lid margin irregularity (range 0–2)	0.6 (0.5)	1.1 (0.7)	0.03*
Telangiectasia (range 0–2)	0.6 (0.5)	1.5 (0.5)	<0.001*
Meibum quality (range 0–4)	0.1 (0.2)	0.6 (0.7)	0.02*
Meibomian gland Expression (range 0–3)	0.4 (0.5)	0.7 (0.7)	0.14
Meiboscore (range 0–4)	0.6 (0.5)	2.0 (0.9)	<0.001*

Note: Data represent the average and standard deviation (SD). p-Values are shown for the differences between the groups.

*Indicates a statistically significant difference.

TABLE 2 Mean contrast (standard deviation) calculated for each eyelid, image contrast and study group.

		K5M C		K5M R		K5M RC	
Michelson		**CIN**	**CINTER**	**CIN**	**CINTER**	**CIN**	**CINTER**
Control	UE	5.0 (0.7)	18 (3)	2.6 (0.7)	6 (1)	5 (1)	14 (3)
	LE	5.3 (0.5)	22 (7)	2.8 (0.5)	7 (1)	6 (1)	19 (3)
Pathology	UE	4.7 (0.6)	15 (4)	2.9 (0.9)	6 (3)	4.3 (0.9)	13 (3)
	LE	4.6 (0.8)	17 (4)	3 (1)	6 (2)	5 (1)	16 (4)
P-Value	UE	0.30	0.01*	0.56	0.72	0.45	0.19
	LE	0.02*	0.001*	0.47	0.20	0.004*	0.007*
Yeh and Lin		**δ CIN**	**δ CINTER**	**δ CIN**	**δ CINTER**	**δ CIN**	**δ CINTER**
Control	UE	18 (3)	56 (12)	8 (2)	17 (2)	16 (4)	43 (9)
	LE	20 (3)	62 (13)	10 (3)	22 (5)	21 (4)	61 (9)
Pathology	UE	16 (3)	46 (12)	7 (1)	16 (3)	14 (4)	39 (11)
	LE	18 (4)	55 (15)	10 (4)	22 (8)	18 (4)	54 (11)
p-Value	UE	0.09	0.01*	0.05*	0.35	0.25	0.11
	LE	0.06	0.04*	>0.99	0.76	0.03*	0.01*

Note: Results were obtained using the Michelson (upper table) and Yeh and Lin contrast (lower table). p-Values compare the control and the pathology group. All measures were made separately for the upper (UE) and lower eyelids (LE).

Abbreviations: K5M C (Oculus Keratograph 5M meibography image with enhanced contrast); K5M R (Oculus Keratograph 5M meibography raw image); K5M RC, Oculus Keratograph 5M meibography raw mage with enhanced contrast; CIN, In-gland contrast with Michelson equation; δ CIN, In-gland contrast with Yeh and Lin equation; CINTER, Inter-gland contrast with Michelson equation; δ CINTER, Inter-gland contrast with Yeh and Lin equation.

*Statistically significant differences ($p < 0.05$).

DISCUSSION

In the present study, contrast differences between a MG pathology group and normal control subjects were analysed to assess a number of instrumental factors regarding the use of contrast as a biomarker for MGD. Those factors, based on the goals outlined in the introduction were: (1) the difference between the Michelson and Yeh and Lin's equations for computing contrast, (2) whether the in-gland and inter-gland contrast are equally useful as a biomarker and (3) the impact of image pre-processing (or more accurately, contrast enhancement) when using contrast to distinguish between normal individuals and those with MGD.

Two measures of contrast were calculated using the classical Michelson equation (Equation 1), and the one used by Yeh and Lin (Equation 2).[22,28] The results for both inter- and intra-glandular contrast were similar for each determinant of contrast, although the *p*-values shown in Table 2 were, on average, lower for the Michelson calculation. Nevertheless, these results suggest that the definitions of contrast are comparable for differentiating between healthy eyelids and those with MGD. For either method of quantifying contrast, when significant differences were found, inter-gland contrast was lower for the pathology group, in both the upper and lower eyelids. As noted by Knop et al.,[1] this may be because MG-related pathologies lead to an alteration in the glands so that they appear blurred or even disappear. To date, no study has assessed the relationship between the MG contrast and its functionality, but it is possible that changes in the MG lead either to a reduction in the production of meibum and/or the meibum is less consistent, resulting in a lower contrast image.

Regarding inter-gland and in-gland contrast, the results show that inter-gland contrast is most useful, as this variable provides greater consistency for discerning between the control and pathology groups. For in-gland contrast, homogeneity in the measurements was not obtained, suggesting that this is a weak biomarker. This is consistent with previous studies such as Yeh and Lin, who evaluated inter-gland contrast and noted significant differences between the control and the MG pathology groups.[22]

It has been observed that the contrast varies with the type of image being processed. Many previous studies[22,28] using the Oculus Keratograph 5M have used the enhanced images (K5M C) provided by the instrument. In both these investigations and the present study, statistically significant differences in these contrast-enhanced images were found between the control and pathology groups. However, this was not the case when using the raw images (K5M R) captured by the instrument. This may be because the instrument camera does not have sufficient dynamic range to discriminate gland contrast properly.

Accordingly, it seems that contrast enhancement is necessary to discriminate between healthy and pathological glands. Applying a generic contrast enhancement algorithm (K5M RC), which simulated the program included with the Oculus K5M, only provided statistically significant differences between the groups for the CIN and CINTER variables in the lower lid. Without knowing the exact details of the contrast enhancement algorithm employed by the Oculus K5M, it is difficult to state why this algorithm gives better results. However, this point should be emphasised. Almost all image processing algorithms are dependent on numerical parameters that determine their performance. In the present work, the standard values of the CLAHE algorithm were maintained, while it may be that the parameters used in the K5M software have been optimised for MG images.[2] Therefore, further study is needed on this point. These results stress the importance of the contrast enhancement algorithm, and particularly optimisation of the algorithm parameters for the MGs.

Other instrumental issues can make it difficult to measure contrast. The anatomy of the inner eyelid and the arrangement of the glands are paramount. The curvature of the eyelid influences the quality of the captured images due to the limited depth-of-field of the instrument (note that MG images are captured in micro-photographic conditions). Thus, if the instrument camera is focused on the central eyelid, then it is difficult to assess contrast in the nasal and temporal areas due to loss of definition. Consequently, the area in which gland contrast is computed should be limited to the central portion of the eyelid. This is confirmed by previous studies on gland segmentation using machine learning techniques.[16,18] The depth at which the glands are located in the eyelid is another variable that directly affects contrast measurements.

Additionally, artefacts, such as glare and flare, produced by the interaction of light, the tear film and the imaging camera influence the quality of the image. Given the results obtained here, it would be of interest to analyse how contrast varies when light filters are used to enhance the contrast of raw images. In addition, further work is needed to extrapolate these results to devices other than the OCULUS Keratograph 5M. In addition to the instrument used to obtain MG image contrast, it would also be valuable to assess possible changes in MG contrast throughout the day for both normal and abnormal participants, to deepen the knowledge of glandular physiology.

In conclusion, this study suggests that measurement of the MG contrast can be a biomarker for pathology, provided adequate testing conditions are adopted. The results indicate that the optimal method to proceed with the OCULUS Keratograph 5M is to measure contrast-enhanced images using the algorithm included in the device's software. However, further clinical and symptomatology testing should be carried out to expand the information for obtaining an accurate diagnosis.

AUTHOR CONTRIBUTIONS

Elena Diz-Arias: Conceptualization (equal); data curation (equal); investigation (equal); visualization (equal); writing – original draft (equal); writing – review and editing (equal). **Elena Fernández-Jiménez:** Conceptualization (equal); investigation (equal); visualization (equal); writing – original draft (equal); writing – review and editing (equal).

Assumpta Peral: Methodology (lead); project administration (lead); supervision (lead); visualization (equal); writing – original draft (supporting); writing – review and editing (supporting). **Jose A. Gómez-Pedrero:** Funding acquisition (lead); methodology (lead); project administration (lead); software (supporting); supervision (lead); visualization (equal); writing – original draft (supporting); writing – review and editing (supporting).

ACKNOWLEDGEMENTS

The authors thank all the study participants and staff at the study site. The authors wish to thank Professors Javier Castro and Cristobal Pareja of the College of Statistics, University Complutense of Madrid for their help in the statistical analysis. Finally, the authors would like to thank Cristina Niño-Rueda, Ophthalmologist, in the Department of Optics and Optometry, for her help in the clinical diagnosis.

FUNDING INFORMATION

This work was supported by the European Fund for Regional Development (EFRD- FEDER, EU) and by the Spanish Government's Agencia Estatal de Investigación through grant DPI2016-75272-R. Elena Diz is supported by a Santander-UCM grant for pre-doctoral research students.

CONFLICT OF INTEREST STATEMENT

The authors declare no conflicts of interest.

ORCID

Elena Diz-Arias https://orcid.org/0000-0003-0317-2054
Elena Fernández-Jiménez https://orcid.org/0000-0003-3500-0388
Assumpta Peral https://orcid.org/0000-0002-7495-3088
Jose A. Gomez-Pedrero https://orcid.org/0000-0001-7043-3256

REFERENCES

1. Knop E, Knop N, Millar T, Obata H, Sullivan DA. The international workshop on Meibomian gland dysfunction: report of the subcommittee on anatomy, physiology, and pathophysiology of the Meibomian gland. *Invest Ophthalmol Vis Sci*. 2011;52:1938–78.
2. Arita R, Fukuoka S, Morishige N. New insights into the morphology and function of Meibomian glands. *Exp Eye Res*. 2017;163:64–71.
3. Nichols KK. The international workshop on Meibomian gland dysfunction: introduction. *Invest Ophthalmol Vis Sci*. 2011;52:1917–21.
4. Geerling G, Baudouin C, Aragona P, Rolando M, Boboridis KG, Benítez-del-Castillo JM, et al. Emerging strategies for the diagnosis and treatment of Meibomian gland dysfunction: proceedings of the OCEAN group meeting. *Ocul Surf*. 2017;15:179–92.
5. Schiffman RM, Christianson MD, Jacobsen G, Hirsch JD, Reis BL. Reliability and validity of the ocular surface disease index. *Arch Ophthalmol*. 2000;118:615–21.
6. Price DD, McGrath PA, Rafii A, Buckingham B. The validation of visual analogue scales as ratio scale measures for chronic and experimental pain. *Pain*. 1983;17:45–56.
7. Paugh JR, Kwan J, Christensen M, Nguyen AL, Senchyna M, Meadows D. Development of a Meibomian gland dysfunction – specific symptom questionnaire. *Eye Contact Lens*. 2018;44:6–14.
8. Pult H, Nichols JJ. A review of meibography. *Optom Vis Sci*. 2012;89:E760–9.
9. Wise RJ, Sobel RK, Allen RC. Meibography: a review of techniques and technologies. *Saudi J Ophthalmol*. 2012;26:349–56.
10. Arita R, Itoh K, Maeda S, Maeda K, Amano S. A newly developed noninvasive and mobile pen-shaped meibography system. *Cornea*. 2013;32:242–7.
11. Pult H, Riede-Pult BH. Non-contact meibography: keep it simple but effective. *Cont Lens Anterior Eye*. 2012;35:77–80.
12. Arita R, Itoh K, Inoue K, Amano S. Noncontact infrared meibography to document age-related changes of the Meibomian glands in a normal population. *Ophthalmology*. 2008;115:911–5.
13. Tomlinson A, Bron AJ, Korb DR, Amano S, Paugh JR, Pearce EI, et al. The international workshop on Meibomian gland dysfunction: report of the diagnosis subcommittee. *Invest Ophthalmol Vis Sci*. 2011;52:2006–49.
14. Saha RK, Chowdhury AMM, Na KS, Hwang GD, Eom Y, Kim J, et al. Automated quantification of Meibomian gland dropout in infrared meibography using deep learning. *Ocul Surf*. 2022;26:283–94.
15. Setu MAK, Horstmann J, Schmidt S, Stern ME, Steven P. Deep learning-based automatic Meibomian gland segmentation and morphology assessment in infrared meibography. *Sci Rep*. 2021;11:7649. https://doi.org/10.1038/s41598-021-87314-8
16. Wang J, Li S, Yeh TN, Chakraborty R, Graham AD, Yu SX, et al. Quantifying Meibomian gland morphology using artificial intelligence. *Optom Vis Sci*. 2021;98:1094–103.
17. Zhang Z, Lin X, Yu X, Fu Y, Chen X, Yang W, et al. Meibomian gland density: an effective evaluation index of Meibomian gland dysfunction based on deep learning and transfer learning. *J Clin Med*. 2022;11:2396. https://doi.org/10.3390/jcm11092396
18. Wang J, Yeh TN, Chakraborty R, Yu SX, Lin MC. A deep learning approach for Meibomian gland atrophy evaluation in Meibography images. *Transl Vis Sci Technol*. 2019;8:37. https://doi.org/10.1167/tvst.8.6.37
19. Prabhu SM, Chakiat A, Shashank S, Vunnava KP, Shetty R. Deep learning segmentation and quantification of Meibomian glands. *Biomed Signal Proc Control*. 2020;57:101776. https://doi.org/10.1016/j.bspc.2019.101776
20. Pult H, Riede-Pult B. Comparison of subjective grading and objective assessment in meibography. *Cont Lens Anterior Eye*. 2013;36:22–7.
21. García-Marqués JV, García-Lázaro S, Martínez-Albert N, Cerviño A. Meibomian glands visibility assessment through a new quantitative method. *Graefes Arch Clin Exp Ophthalmol*. 2021;259:1323–31.
22. Yeh TN, Meng CL. Meibomian gland contrast sensitivity and specificity in the diagnosis of lipid-deficient dry eye: a pilot study. *Optom Vis Sci*. 2021;98:121–6.
23. Peral A, Alonso J, Gomez-Pedrero JA. Effect of illuminating wavelength on the contrast of meibography images. *OSA Continuum*. 2018;1:1041–54.
24. Alghamdi WM, Markoulli M, Holden BA, Papas EB. Impact of duration of contact lens wear on the structure and function of the Meibomian glands. *Ophthalmic Physiol Opt*. 2016;36:120–31.
25. Zuiderveld K. Contrast limited adaptive histograph equalization. In: Heckbert PS, editor. Graphic gems IV. San Diego: Academic Press Professional; 1994. p. 474–85.
26. Diz-Arias E, Fernandez-Jimenez E, Peral A, Gomez-Pedrero JA. Code for computing Meibomian gland contrast. 2022 GitHub. https://github.com/InforUCM/ContrasteMG. Accessed 24 April, 2023.
27. Senthilkumaran N, Kirubakaran C. Efficient implementation of Niblack thresholding for MRI brain image segmentation. *Int J Comp Sci Inform Technol*. 2014;5:2173–6.
28. Yeh TN, Meng CL. Repeatability of Meibomian gland contrast, a potential indicator of Meibomian gland function. *Cornea*. 2019;38:256–61.

How to cite this article: Diz-Arias E, Fernández-Jiménez E, Peral A, Gomez-Pedrero JA. Role of instrumental factors in Meibomian gland contrast assessment. *Ophthalmic Physiol Opt*. 2023;00:1–9. https://doi.org/10.1111/opo.13156